Available online at http://www.ifgdg.org

Int. J. Biol. Chem. Sci. 12(2): 1008-1027, April 2018

International Journal of Biological and Chemical Sciences

ISSN 1997-342X (Online), ISSN 1991-8631 (Print)

Original Paper http://ajol.info/index.php/ijbcs http://indexmedicus.afro.who.int

Nicotinic acid as green inhibitor for copper corrosion in 3.5 wt % NaCl solution: experimental and quantum chemical calculations

Nagnonta Hippolyte COULIBALY[1], Yapi Serge BROU[1*], Gbé Didier DIOMANDE[2], Juan CREUS[3] and Albert TROKOUREY[1]

[1]*Laboratoire de Chimie Physique (LCP), Université Félix Houphouët-Boigny d'Abidjan, 22 BP 582 Abidjan 22, Côte d'Ivoire.*
[2]*Laboratoire de Chimie Organique et de Substances Naturelles (LCOSN), Université Félix Houphouët-Boigny d'Abidjan, 22 BP 582 Abidjan 22, Côte d'Ivoire.*
[3]*Laboratoire des Sciences de l'Ingénieur pour l'Environnement (LaSIE) UMR 7356 CNRS, Université de La Rochelle, Avenue Michel Crépeau 17042 La Rochelle Cedex 1, France.*
[*]*Corresponding author; E-mail: lesaintbys@yahoo.fr; Tel: +225 49 37 95 44; 22 BP 582 Abidjan 22, Côte d'Ivoire.*

ABSTRACT

This work reports the inhibition properties of nicotinic acid (NAC) for copper protection during its applications in seawater systems such as water pipelines, shipbuilding, seawater desalination operations and heat exchange systems. The efficiency of nicotinic acid (NAC) as a copper corrosion inhibitor in 3.5 wt % NaCl solution was investigated by Tafel extrapolation and electrochemical impedance spectroscopy (EIS) methods in the temperature range from 20 to 50 °C. The corrosion parameters and the adsorption isotherms were determined from the potentiodynamic polarization curves. It was found that the inhibitory efficiency (η%) and the coverage rate (θ) increase to a maximum of 87.97 at 25 °C in 10 mM of nicotinic acid at fixed temperature but decrease as the temperature of the solution increases. Nicotinic acid acts is a purely cathodic inhibitor. Moreover, the obtained thermodynamic parameters using Langmuir model suggested a physical adsorption type. A correlation was found between the corrosion inhibition efficiency and the theoretical parameters obtained by the functional density method B3LYP/ 6-31 + G (d, p). All these results indicate that the addition of NAC in the corrosive solution significantly decreases the corrosion rate.

Keywords: Nicotinic acid, copper corrosion inhibition, electrochemical impedance spectroscopy, quantum chemical calculations.

INTRODUCTION

The problem of corrosion is of great concern since the repair of the resulted structures has been proved to be an expensive process. Aqueous corrosion affects virtually all areas of human activity from buildings to installation and equipment, especially petroleum installations and materials in contact with seawater. The economic importance of corrosion metals is no longer to be demonstrated. It is estimated that corrosion destroys one-quarter of the world's annual

DOI : https://dx.doi.org/10.4314/ijbcs.v12i2.30

steel production, which is about 150 million tons per year (Mansouri, 2015). To overcome this problem, the most commonly used inhibitors are organic molecules. These compounds can adsorb on metal surface and block the active surface sites to reduce the corrosion rate. Four types of adsorption take place by organic molecules at metal/solution interface : (a) electrostatic attraction between the charged molecules and charged metal, (b) interaction of uncharged electron pairs in the molecule with the metal, (c) interaction of π-electrons with the metal and (d) combination of (a) and (c) (Ostovari et al., 2009). Upon incorporation of the inhibitor into the electric double layer on the metal surface, the polarized molecule or inhibitor ion changes the charge distribution, and consequently the electrical potential (Yingchu et al., 1996; Aksüt, 1997; Stoyanova et al., 1997). In this context, considerable efforts are being made to find the appropriate compounds to be used as corrosion inhibitors in order to stop or delay the attack of a metal as much as possible. Several studies have been carried out using heteroatom (nitrogen, oxygen, sulfur …) compounds and have shown that these inhibitors have good inhibitory efficiency on different materials and in different corrosive media (El Ouafi et al., 2002; Tourabi et al., 2014). However, most of them are found to have toxic effects to living organism and are harmful to the environment. Due to environmental concerns, vitamins are increasingly being considered as "green" corrosion inhibitors. Vitamins B2 (Riboflavin) (Chidiebere et al., 2015), B1 (Thiamine) (Niamien, 2016) have been used for the protection of copper in an acid medium.

Third vitamin of class B, nicotinic acid (C_5H_4NCOOH) or niacin or vitamin B3 (Figure 1) is a micro-heterocyclic compound containing a nitrogen atom, with a carboxyl group and π bonds. These characteristics are considered to be important factors for a good inhibition effects. In addition, nicotinic acid is very cheap, readily available and non-toxic.

Ju and Li (2007) and Kanojia and Singh (2005) studied the corrosion of Zn-Al alloy inhibition in the presence of nicotic acid in hydrochloric acid medium and the steel in sulfuric acid medium. According to their results, nicotinic acid protects various studied metals against corrosion. It is found that it is a mixed-type inhibitor which effectiveness increases with concentration and decreases as the temperature increases. In addition, it acts by adsorption on the metal surface following the Langmuir adsorption isotherm. Such results have inspired us to test this molecule in the case of copper in NaCl solution. This work aimed at studying the effects of nicotinic acid on copper corrosion in a 3.5 wt % NaCl solution. The effect of inhibitor concentration, immersion time and temperature were also investigated. In addition to the used techniques (electrochemical polarization, electrochemical impedance spectroscopy), quantum chemical calculations and surface analyzes of the tested samples were carried out.

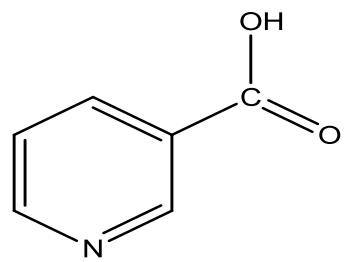

Figure 1: Molecular structure of nicotinic acid (NAC)**.**

MATERIALS AND METHODS

Samples

The cylindrical samples of copper with a purity of 99.9% are mounted in glass tubes of suitable diameter to provide an exposed active geometrical surface area of 3.14 cm^2 to the corrosive medium. Prior to each test, copper substrates were grinded with abrasive papers of decreasing particle size (400, 800, 1000, 1200 and 2000), rinsed with Milli-Q water (18.2 MΩ·cm), degreased with ethanol and then rinsed again with Milli-Q water and dried in air.

Solutions

The corrosive medium consists of a 3.5 wt % sodium chloride solution which is obtained by dissolving Sigma-Aldrich sodium chloride (99.5%) in deionized water. The analytical nicotinic acid was purchased from Sisco Research Laboratories Pvt. Ltd. The solutions of concentrations ranging from 1 to 50 mM were prepared by dilution. All tests are carried out in solutions with magnetic and aerated stirring. A Thermo-cryostat Lauda model E100 permits to keep the electrolyte at the fixed temperature.

Electrochemical measurements

The electrochemical measurements were performed in a three-electrode cell with a volume of 0.5 L. The working electrode (WE) was copper samples, the counter electrode (CE) was a platinum wire, and the reference (Ref) electrode was a saturated calomel electrode (SCE: 0.241 V vs SHE). The electrochemical study (Electrochemical impedance spectroscopy (EIS), potentiodynamic, and linear polarization) of the behavior of copper in contact with the corrosive medium in the absence or in the presence of inhibitor is carried out using an experimental device composed of a Potentiostat-Galvanostat MODULAB, a DELL computer equipped with MODULAB XM ECS software allowing data processing.

Potentiodynamic polarization measurements

The potentiodynamic current–potential curves were recorded by changing the electrode potential automatically from -300 to 150 mV with a scanning rate of 0.2 mV s^{-1}. The polarization resistance measurements were performed by applying a controlled potential scan over a small range, typically ±20 mV with respect to E_{corr}. The resulting current is linearly plotted versus potential; the slope of this plot at E_{corr} being the polarization resistance (Rp).

Electrochemical impedance spectroscopy (EIS)

The impedance measurements are carried out at 25 °C after 60 minutes of immersion in 3.5 wt % NaCl solution with or without inhibitor. The amplitude of the applied sinusoidal voltage to the drop potential is 10 mV peak-to-peak at frequencies between 10^{-2} and 6.10^4 Hz with 10 points per decade. Impedance data has been analyzed and fitted by using ZView2.3 impedance software. All the impedance diagrams were performed in potentiostatic mode at the open circuit potential and presented in the Nyquist diagram (Re-jIm) where Re is the real and -jIm is the imaginary part in Bode plane.

Surface Analysis

Raman Spectroscopy

Raman spectroscopy measurements were performed using a Jobin Yvon Horiba high resolution spectrometer (LabRam HR8000 model) with a monochromatic He-Ne laser source of wavelength λ = 632.817 nm. Spectrum processing is performed using Jobin Yvon's LabSpec software.

Optic microscopy

The morphology of the sample surface after immersion of 72 h in the 3.5 wt % NaCl solution with and without inhibitor was analyzed with a LEICA DM6000 M optical microscope equipped with LAS V4.9 software.

Quantum chemical calculations

For the theoretical study, the complete geometry of the molecule has been optimized in the functional theory of density by the functional hybrid B3LYP (Becke 3 parameters Lee Yang Parr) with the orbitals base 6-31 + G (d, p) using Gaussian 03 W software (Frisch et al., 2003). The quantum chemical

parameters obtained from this optimized structure are: the energy of the highest occupied molecular orbital (E_{HOMO}) and the lowest unoccupied (E_{LUMO}), the difference (the gap) $\Delta E = E_{LUMO} - E_{HOMO}$, the dipole moment ($\mu$) and the Mulliken charges on the heteroatoms. Parameters such as ionization potential (I), electronic affinity (A), electronegativity (χ), overall hardness (η) and fraction of transferred electrons (ΔN) were also calculated.

RESULTS

Open circuit potential

The open circuit potential is the most immediately measurable electrochemical parameter. This simple technique provides preliminary information on the nature of current processes at the metal/electrolyte interface: corrosion, passivation. Figure 2 presents the evolution of open circuit potential of the copper electrode in a 3.5 wt % NaCl solution with and without inhibitor.

In blank solution, the open circuit potential of the copper electrode slightly evolves from -220 to -255 mV/SCE during the first hours of immersion. We can observe some small potential fluctuations during the immersion. A slight shift of the open circuit potential towards more negative values was also observed.

In the presence of NAC, the open circuit potential is shifted toward more negative potential values compared with the blank solution. During the immersion, the open circuit potential evolves towards more positive values.

Potentiodynamic polarization curves

Figure 3 shows the polarization curves of the copper in an aerated 3.5 wt % NaCl solution without and with addition of the NAC at different concentrations. The polarization curves were plotted after one hour of immersion in saline solution.

In the blank solution, the corrosion potential is around -220 mV/SCE. In the cathodic domain, it can be observed a first regime up to -340 mV/SCE where a linear variation of the current density versus potential is noticed. For higher cathodic overpotentials, a reduction peak is observed. A linear variation of the current density versus potential is observed in the anodic domain. With the addition of inhibitors, the shape of the polarization curves is quite similar. An increase in NAC concentration leads to a shift of the corrosion potential towards more cathodic potentials. This displacement is associated with a remarkable drop of the current density compared with that obtained in a blank solution with a modification of the cathodic Tafel slope values.

It can also be noted that the anodic polarization curves are not drastically affected by the presence of the NAC, a slight modification of the anodic slope is observed with the presence of the inhibitor species.

The Electrochemical parameters such as corrosion potential (E_{corr}), anodic (ba), and cathodic (bc) Tafel slopes and the corrosion current density (j_{corr}) are determined by Tafel extrapolation method of potentiodynamic polarization curves. The values are in Table 1**.** The current density was used to calculate the copper corrosion rate (CR) and the inhibitor efficiency (η) using the equations 1 and 2:

$$CR(mm/year) = \frac{3.280 \times j_{corr} \times M_{Cu}}{n \times \rho_{Cu}} \quad (1)$$

$$\eta = \frac{j_{corr} - j_{corr}^{inh}}{j_{corr}} \times 100 \quad (2)$$

j_{corr} et j_{corr}^{inh} (mA/cm^2) are the corrosion current densities of the copper after immersion in 3.5 wt % NaCl medium without and with addition of inhibitor respectively. M_{Cu} (g / mol) is the molar mass of copper, ρ_{Cu} (g / cm^3) the copper density and n is the number of exchanged electrons during the reaction. The polarization resistance was calculated from the Stern-Geary equation:

$$R_P = \frac{b_a \times b_c}{2.303(b_a + b_c)\, j_{corr}} \quad (3)$$

ba and bc are the Tafel slopes.

Long-term immersion measurements

The concentration of 10 mM seems to be the optimal concentration of NAC according to the potentiodynamic polarization study. Long-term immersion measurements at the open circuit potential were performed and polarization resistance test was also scheduled in order to follow the dissolution kinetic. In Figures 4 and 5, it is possible to observe the open circuit potential and polarization resistance of copper as a function of time in the corrosive solution without and with 10 mM of NAC. In the blank solution, the open circuit potential increases slightly up to a maximum at around 35 h of immersion and then slightly decreases. When the tests are conducted in the presence of NAC, an important shift of the potential in the first hours of immersion is observed. This shift is in good agreement with the potentiodynamic experiments and is directly linked to the action mechanism of the inhibitor. After few hours of immersion, the open circuit potential gradually increases.

Furthermore, Figure 5 displays the evolution of the polarization resistance during the extended immersion test. In absence of inhibitor, the polarization resistance increases up to 25 h and after 25 h of immersion, an important decrease of the Rp is observed. In the presence of inhibitor, a continuous increase of polarization resistance is observed during the immersion time.

Electrochemical impedance spectroscopy (EIS)

Electrochemical impedance spectroscopy is a non-stationary (transitory) method which provides information on the elementary steps that constitute the overall electrochemical process. It has several advantages. It allows precise determination of the corrosion rate even in the case where the metal is covered with a protective layer. It also makes it possible to evaluate the rate of inhibition, the characterization of the various steps implied in the global corrosion phenomena (dissolution, passivation, pitting, etc.) and the study of the reaction mechanisms at the electrochemical interface.

In order to confirm the protection efficiency of NAC, electrochemical impedance spectroscopy (EIS) was used at the corrosion potential. The results after 1 hour of immersion in the corrosive solution without and with different concentrations of NAC are displayed in Figure 6.

Nyquist diagrams have two badly separated capacitive loops: one at low frequency which is attributed to the resistance of adsorbed species due to adsorption of the inhibitor molecules on the copper surface and all other accumulated products, while at middle-frequency one typically capacitive loop attributed to double layer capacitance and charges transfer resistance is obtained. The diameter of the capacitive loops increases with the concentration of NAC. Bode absolute impedance plot (Figure 6b) shows that the impedance increases greatly over the whole frequency range with the incremental concentration of nicotinic acid.

Because of the bad separation of loops and to further analyze the impedance spectra, an equivalent electrical circuit with two-time constant elements often used for copper in neutral media (Gerengi et al., 2016) was used to fit the impedance data. This circuit is shown in Figure 7 where Rs is the resistance of the solution between the working electrode and the reference electrode, R_f is the resistance of the adsorbed film formed on the copper surface, and R_{ct} represents the charge transfer resistance linked to the dissolution of copper. The constant phase element CPE_f is composed of the capacitance C_f and the deviation parameter n_1. The Cf capacity is mainly due to the dielectric nature of the surface film (corrosion products and/or adsorbed inhibitor film). The CPE_{dl} is composed of the double layer capacitance C_{d1} and the deviation parameter n_2.

The impedance of CPE is described as follows (Córdoba-Torres et al., 2012)**:**

$$Z_{CPE} = \left[Q(jw)^n \right]^{-1} \quad (4)$$

where Q is the magnitude of the CPE, j is the imaginary root, w is the angular frequency, n

is the deviation parameter in regard to phase shift. For values of n = 1, 0, -1, CPE is identical to capacitor element (C), resistance (R) and inductance (L) respectively.

However, the effective double layer capacitance (C) derived from the CPE parameters was calculated from the Brugg equation (10) (Córdoba-Torres et al., 2012):

$$C_{CPE_{dl}} = \left[Q(R_S^{-1} + R_{ct}^{-1})^{(n-1)}\right]\frac{1}{n} \quad (5)$$

The inhibition efficiency is calculated from the values of the polarization resistance R_P ($R_p = R_f + R_{ct}$) using Eq.6:

$$\eta = \frac{R_p^{inh} - R_p}{R_p^{inh}} \times 100 \quad (6)$$

The values of the electrochemical parameters and the inhibition efficiency (E%) for different concentrations of inhibitor obtained by electrochemical impedance spectroscopy are presented in the Table 2. This table shows that the values of charge transfer resistance (Rct) and inhibition efficiency (EI) increase with the concentration of NAC to reach a maximum at the 10 mM. It is also noted that the double-layer capacitance exhibits a contrary evolution to the two preceding quantities.

Adsorption isotherm studies

Inhibition by organic molecules is generally due to their adsorption on metal surface. Information on interactions between the inhibitor and metal surface can be studied using adsorption isotherms. The curve of Cinh /θ as a function of the Cinh (inhibitor concentration) is shown in Figure 8. The obtained graph is substantially linear at the study temperature, indicating that the adsorption of NAC on the surface of the copper obeys the Langmuir adsorption isotherm described by Equation 7 (Villamil et al., 1999):

$$\frac{C_{inh}}{\theta} = \frac{1}{K_{ads}} + C_{inh} \quad (7)$$

However, there is a slight deviation of the value of the slope from unity (Table **3**). Therefore, the corrected Langmuir model is more suitable for NAC compound adsorption. The deviation of the value of the slope from unity is due to the interactions between the adsorbed species on the metal surface. The modified Langmuir model takes into account the interactions between the adsorbed species. The modified Langmuir equation is as follow (Villamil et al., 1999):

$$\frac{C_{inh}}{\theta} = \frac{n}{K_{ads}^{'}} + nC_{inh} \quad (8)$$

Where n is the slope of the straight line corresponding to the Langmuir isotherm.

$$\theta(theta) = \frac{j_{corr} - j_{corr(inh)}}{j_{corr}}$$

is the coverage rate and K_{ads} is the equilibrium constant of the adsorption process related to the free enthalpy of adsorption by the equation 9 (Vashi and Champaneri, 1997) :

$$\Delta G_{ads}^0 = -RT \ln 55.5 K_{ads} \quad (9)$$

The determined values of K_{ads} and ΔG_{ads}^0 have been recorded in Table **3**. These K_{ads} value is higher. This high value indicates that the adsorbed layer on the copper surface is stable (Benali et al., 2005). It is known in the literature (Gomma and Wahdan, 1995) that values close to or greater than -20 kJ.mol^{-1} are generally related to interactions between charged molecules and metal charges (physisorption). On the other hand, the values around or especially less than -40 kJ.mol^{-1} is attributed to a transfer of charges between the molecules of the inhibitor and the surface of the metal (chemisorption) with the formation of covalent or coordination bonds. In the present work, the value of ΔG_{ads}^0 = -34.09 kJ.mol^{-1} could allow the two modes of adsorption (chemisorption and physisorption) to be considered.

Effect of temperature

Temperature is one of the factors that can modify the behavior of materials in a

given corrosive medium as well as the inhibitory efficiency of a compound. Considering the importance of this factor, we have carried out potentiodynamic polarization tests of copper in the 3.5 wt % NaCl without and with addition of 10 mM NAC inhibitor in a temperature range from 20 °C to 50 °C. The obtained curves are shown in Figure 9. The E_{corr} and j_{corr} values obtained from these curves are shown in Table 4.

Considering the result in Figure 9, the increase in temperature leads to an increase in the current density both in the absence and presence of the NAC inhibitor. The decrease in inhibition efficiency with increasing temperature as observed in Table 4 is suggestive of physisorption mechanism generally attributed to electrostatic interaction between charged molecules and charged metal. This observation can be interpreted by the reduction in stability of the adsorbed film at higher temperature. According to Obot and Obi-Egbedi, as temperature increases, Gibbs free energy and change in enthalpy rise to a higher value, so that some of the chemical bonds joining the molecules onto the metallic surface are impaired and the film stability reduced. It may further be attributed to a possible shift of the adsorption/desorption equilibrium towards desorption of adsorbed inhibitor due to increasing solution agitation. Thus, as the temperature increases the number of adsorbed molecules decreases, leading to a decrease in the inhibition efficiency (Obot and Obi-Egbedi, 2011).

We note that the study of the effect of temperature can inform us about the type of adsorption of the inhibitor on the surface of the metal (chemisorption or physisorption) by the determination of the activation energy (E_a), the enthalpies (ΔH_a) and entropy (ΔS_a) of activation of the corrosion process. The Arrhenius dependence between the density of the corrosion current and the temperature allowed us to calculate the energy of activation in the absence and in the presence of inhibitor using the following relation:

$$j_{corr} = k\, exp\left(-\frac{E_a}{RT}\right) \qquad (10)$$

For the determination of ΔH_a and ΔS_a we have used the alternative formula of the Arrhenius equation (11):

$$\log\left(\frac{j_{corr}}{T}\right) = \left[\log\left(\frac{R}{Nh}\right) + \frac{\Delta S_a}{2.303R}\right] - \frac{\Delta H_a}{2.303RT} \qquad (11)$$

where R ($J.mol^{-1}.K^{-1}$) is the perfect gas constant, h (J.s) the Planck constant, T (K) the absolute temperature, N (mol^{-1}) the number of Avogadro and k the pre-exponential factor of Arrhenius.

Figure 10 shows the curves $\ln j_{corr} = f\left(\frac{1000}{T}\right)$ and $\log\left(\frac{j_{corr}}{T}\right) = f\left(\frac{1000}{T}\right)$. The activation parameters recorded in Table 5 were determined.

In our investigations, the activation energy found in presence of NAC is higher than that obtained in its absence, so the adsorption of the studied molecule onto the copper surface is found to be physical in nature (Szauer and Brandt, 1981). The positive sign ΔH_a shows the endothermic nature of the copper dissolution process. The increase in the enthalpy value after the addition of NAC indicates that in the presence of inhibitory molecules, the dissolution of the metal is more difficult (Li et al., 2011). For the negative sign of the activation entropy both in the solution with and without an inhibitor, it can be attributed to the disorder created by the inhibitory molecules on the surface of the metal. The adsorption of adsorbate on the metal surface is regarded as a substitutional adsorption process between the organic compound in the aqueous phase and water molecule adsorbed on the metal surface. The adsorption of inhibitors on the copper surface would be in equilibrium with the desorption of surface wate r molecules:

$$Org_{(sol)} + xH_2O_{(ads)} \rightarrow Org_{(ads)} + xH_2O_{(sol)} \qquad (12)$$

where $Org_{(sol)}$ and $Org_{(ads)}$ are the adsorbates in the bulk solution and adsorbed

on the surface respectively; $H_2O_{(ads)}$ and $H_2O_{(sol)}$ are water molecules adsorbed on the surface and in the solution respectively.

Surface analysis

Micro-Raman Spectroscopy

The surface of specimens exposed to NaCl 3.5 **wt** % solution without and with 10 mM of NAC for 72 hours were examined using ex-situ Raman spectroscopy. In the case of the immersion without inhibitor, the Raman spectrum (Figure 11) shows the existence of cuprite which is a cuprous oxide of formula (Cu_2O). In the presence of the NAC no corrosion products have been detected. NAC has therefore protected copper against corrosion.

Optic microscopy

Figure 12 shows the picture of the copper samples after immersion in a 3.5 **wt** % NaCl solution for 72 h at 298 K in the without and inhibitor (10 mM). The surface of the sample in the absence of the inhibitor (Figure 12b) is strongly corroded if compared with the fresh grinded surface. The corrosion products cover virtually the entire surface of the metal. In the presence of NAC (Figure 12c), the surface of the electrode is well protected and almost identical to that of the freshly polished surface (Figure 12a). We observe that the grinded scratches are present on the surface of the samples after polishing and those after immersion in a 3.5 wt % NaCl solution containing the NAC. Some precipitates at the surface are identified as NaCl crystals appear because of insufficient surface rinsing. The comparison of these three figures reveals a marked inhibiting efficiency of NAC.

Quantum chemical calculations

Quantum chemical calculations were carried out to study the mechanism of adsorption and inhibition of the molecule studied in functional theory of density by the hybrid functional B3LYP (Becke 3 parameters Lee Yang Parr) with the 6-31 + G (d, p) basis set using Gaussian 03 W software. This theoretical study of the nicotinic acid molecule has been carried out with a view to highlight the factors which may favor its inhibitory nature. The calculated chemical parameters include the energy of the highest occupied (E_{HOMO}) and lowest unoccupied (E_{LUMO}) molecular orbital, the difference $\Delta E = E_{LUMO}-E_{HOMO}$, the dipole moment ($\mu$) and the charges of Mulliken on heteroatoms. Parameters such as ionization potential (I), electronic affinity (A), electronegativity (χ), global hardness (η) and fraction of transferred electrons (ΔN) were also calculated using the following relationships (Petrović Mihajlović et al., 2017):

$$I = -E_{HOMO} \quad (13)$$

$$A = -E_{LUMO} \quad (14)$$

$$\chi = \frac{1}{2}(I + A) \quad (15)$$

$$\eta = \frac{1}{2}(I - A) \quad (16)$$

$$\Delta N = \frac{\chi_{Cu} - \chi_{inh}}{2(\eta_{Cu} + \eta_{inh})} \quad (17)$$

The determined values of χ_{Cu} and η_{Cu} in the literature are 4.48 eV and 0 eV, respectively(El Ibrahimi et al., 2016). Figure 13 shows the Optimized molecular structure (left) and mulliken charge distribution (right) of nicotinic acid (NAC). It can therefore be easily seen that the oxygen, nitrogen and the atoms of the aromatic ring carry a high density of negative charges and could therefore constitute active adsorption sites.

Analyzing Figure 14, we can observe that HOMO and LUMO densities are concentrated in nearly the same region, around the following atoms: oxygen, nitrogen and the atom of the aromatic ring, indicating that they are potential active centers for donor-acceptor interactions. The favorable sites for interactions with the surface of the metal are located in these regions (Martinez and Štagljar, 2003). HOMO energy is often associated with the ability of a molecule to give electrons, while LUMO energy indicates its ability to accept electrons. The binding capacity of the inhibitor to the metal surface (Popova et al., 2003) increases with increasing

the HOMO value and decreasing the LUMO energy value. The quantitative parameters of quantum chemistry and reactivity are collected in Table 6. The energy gap ($\Delta E = E_{LUMO}-E_{HOMO}$) is an important parameter as a function of reactivity of the inhibitor molecule towards the adsorption on the metallic surface. Lower values of the energy gap will render good inhibition efficiency, because the energy to remove an electron from the last occupied orbital will be low. In our case, the low value of 5.4037 eV could explained the good inhibition efficiency of nicotinic acid when compared with that of many molecules in the literature (Ju and Li, 2007).

It is known that the value of the dipole moment (μ) characteristic of the hydrophobicity of the molecule decreases when the efficiency of the inhibition increases, suggesting that molecules with weak dipole moments will be easily adsorbed on the metal surface. Similar results can be found in the literature, although several authors state that the inhibitory efficiency increases with the increasing values of the dipole moment. In fact, a review of the literature (Khaled et al., 2005) reveals several irregularities in the case of the correlation between the dipole moment and the inhibitory efficiency. In general, there is no significant relationship between the value of the dipole moment and the inhibitory power of a molecule. The parameter ΔN, the number of electrons transferred, also known as the ability to exchange electrons, indicates the tendency of a molecule to give electrons to the metal surface if $\Delta N > 0$ and the opposite if $\Delta N < 0$ (Petrović Mihajlović et al., 2017). That is to say that the NAC molecule receives the electrons from the copper metal surface.

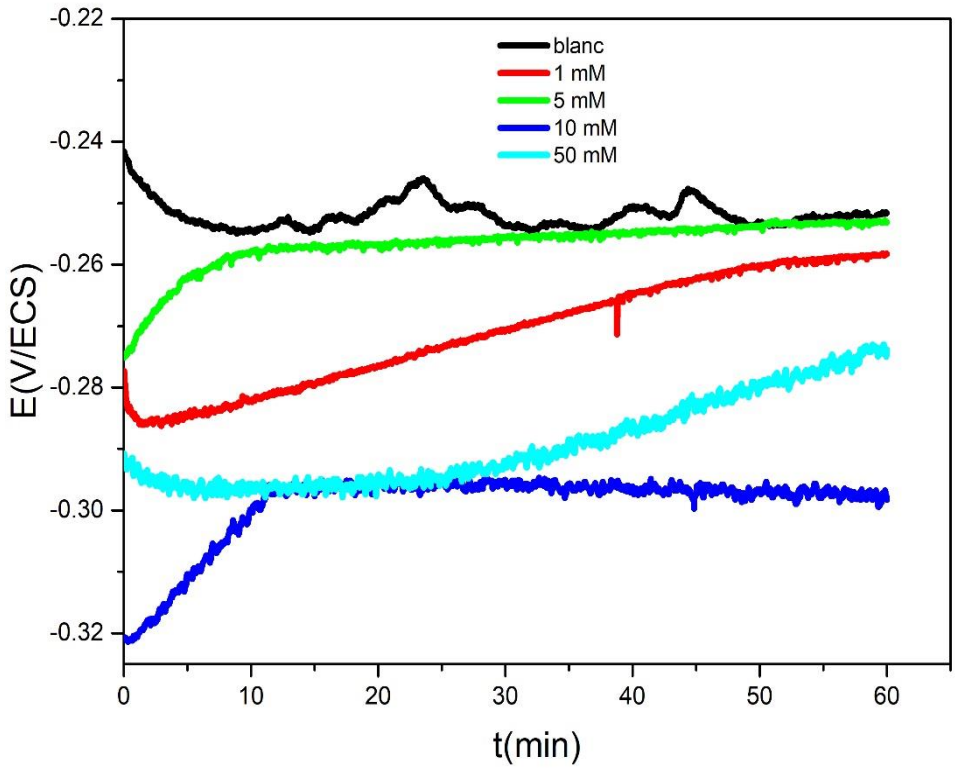

Figure 2 : Open circuit potential-time curves for copper in 3.5 wt % NaCl solution without and with differents concentrations of nicotinic acid.

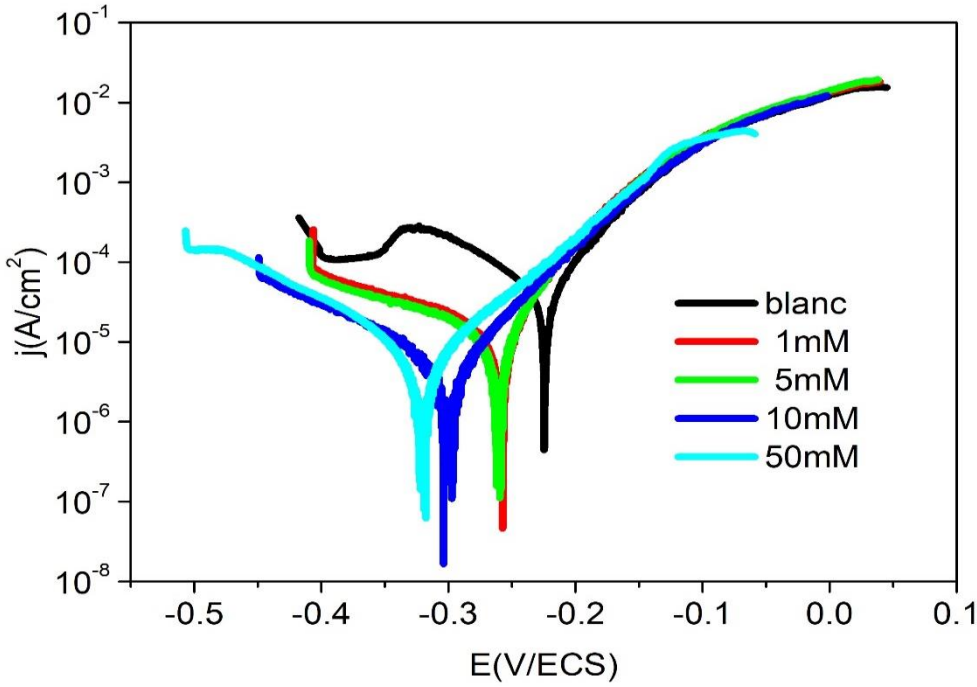

Figure 3 : Potentiodynamic polarization curves for copper in 3.5 wt % NaCl in the without and with nicotic acid.

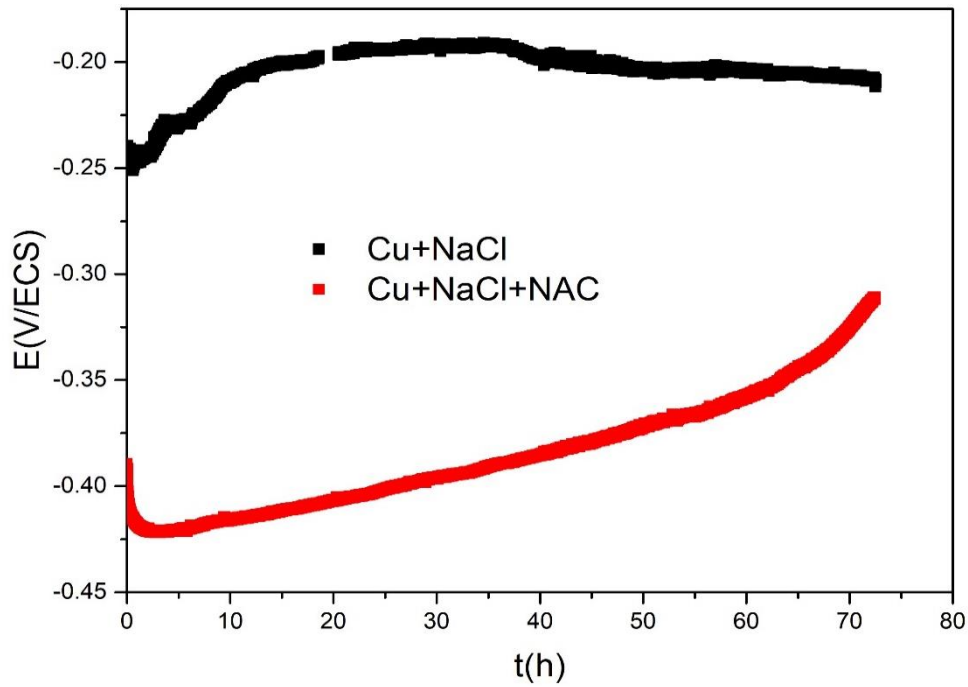

Figure 4 : Open circuit potential versus time curves of copper for 72 h in 3.5 wt % NaCl solution without and with 10 mM of NAC.

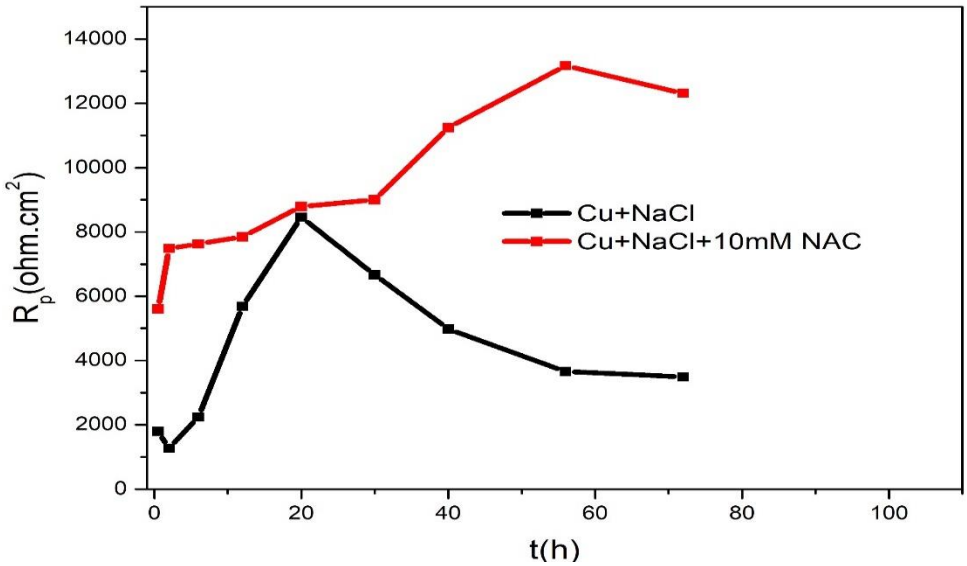

Figure 5 : Evolution of polarization resistance with time, during the immersion in aggressive solution: without and with 10 mM of NAC.

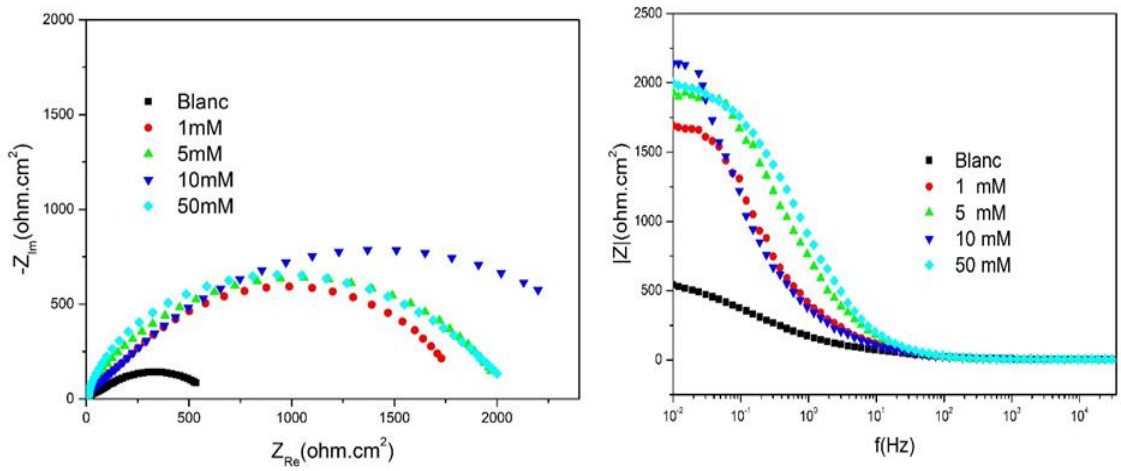

Figure 6: EIS plots for copper in 3.5 wt % NaCl solution without and with different concentrations of NAC at 298 K in (a) Nyquist representation and (b) Bode modulus.

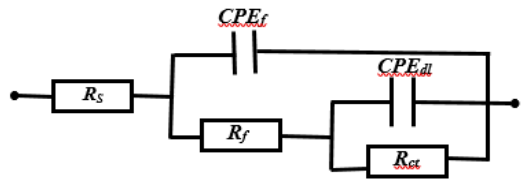

Figure 7: Electrochemical equivalent circuit used to fit impedance data.

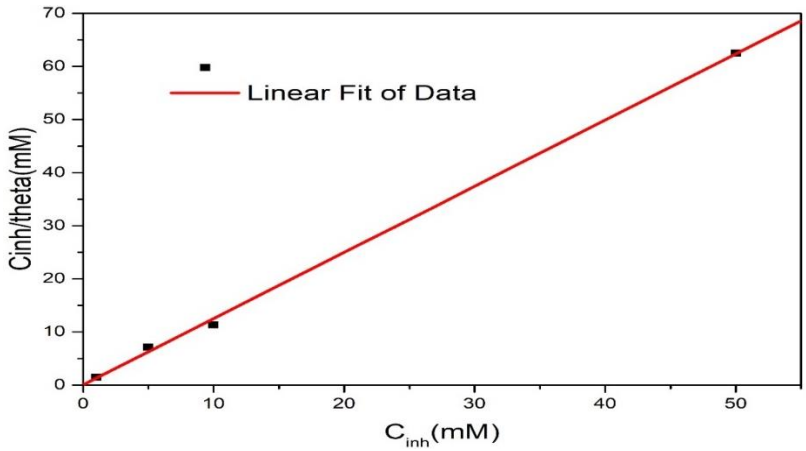

Figure 8 : Langmuir adsorption isotherms of NAC on the copper surface in 3.5 wt % NaCl solution at 298 K.

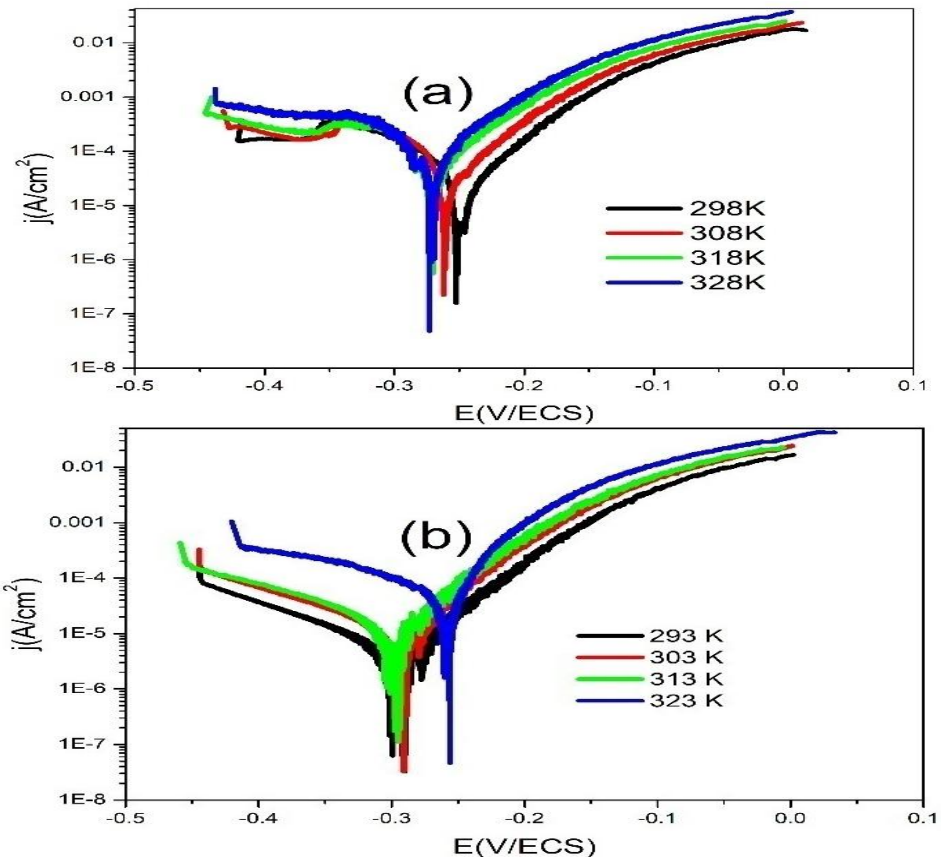

Figure 9 : Polarization curves of copper in NaCl 3.5 wt % solution without inhibitor (a) and with 10 mM of NAC (b) at differents temperatures after 1 h immersion.

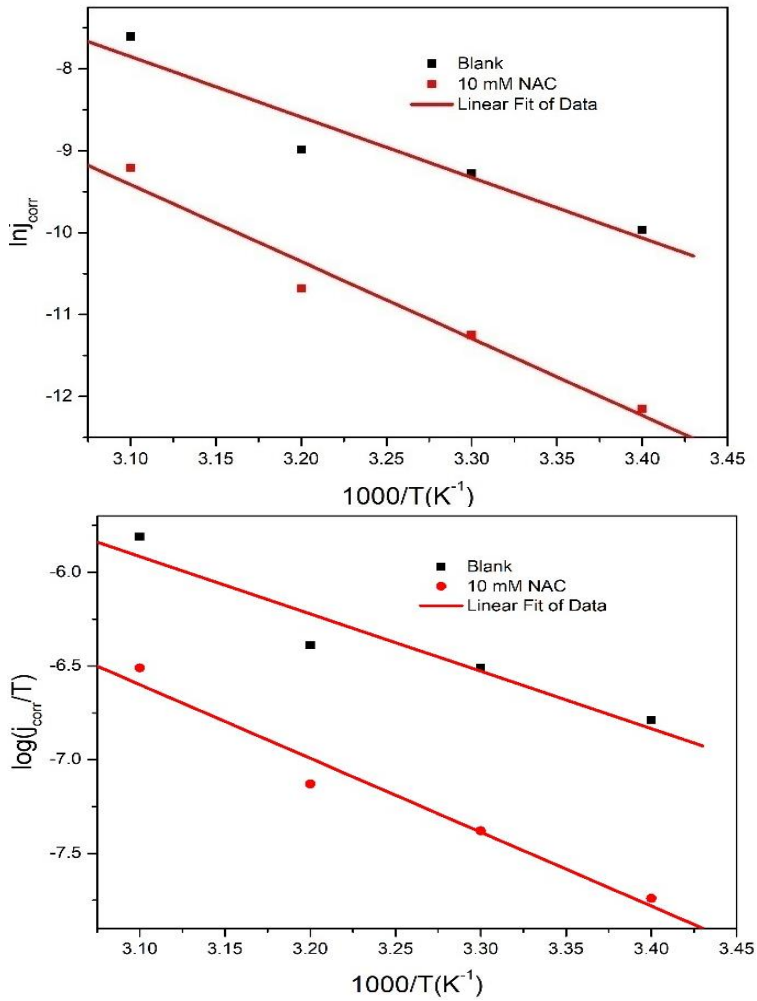

Figure 10 : Arrhenius plot of Ln(j_{corr}) and Transition state plot of Log(j_{corr}/T) versus 1000/T for copper corrosion in NaCl 3.5 wt % without and with 10 mM of NAC.

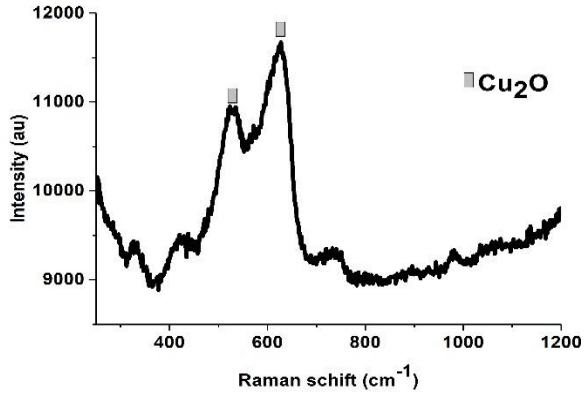

Figure 11: Raman spectra of copper in 3.5 wt % NaCl without nicotic acid after 72 hours of immersion.

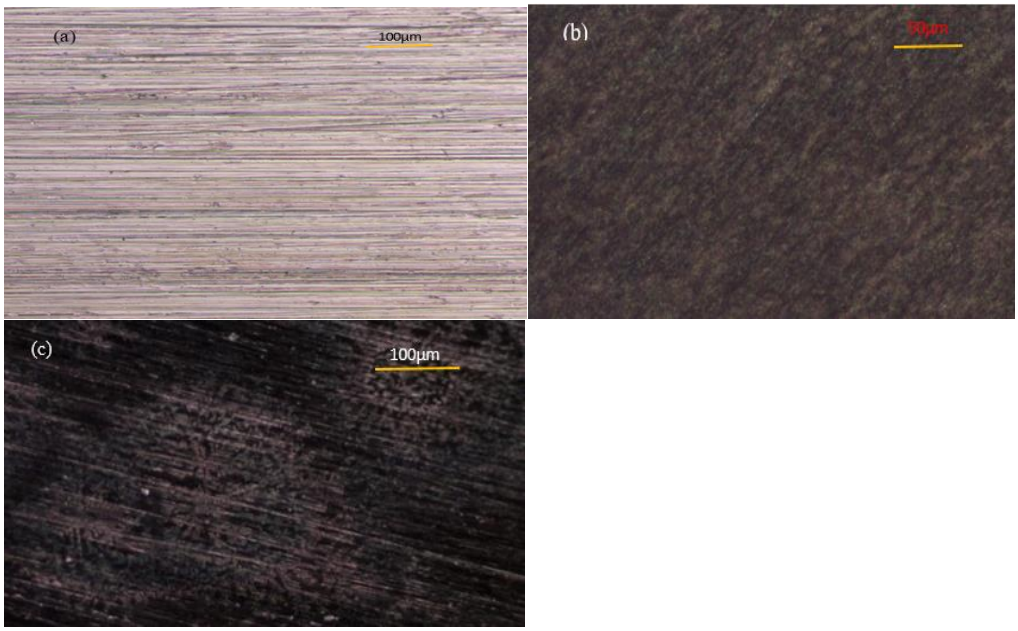

Figure 12: Pictures of the copper surface: a) freshly polished; b) after immersion in blank solution; (c) after immersion (t = 72 hours) in solution with 10 mM of NAC.

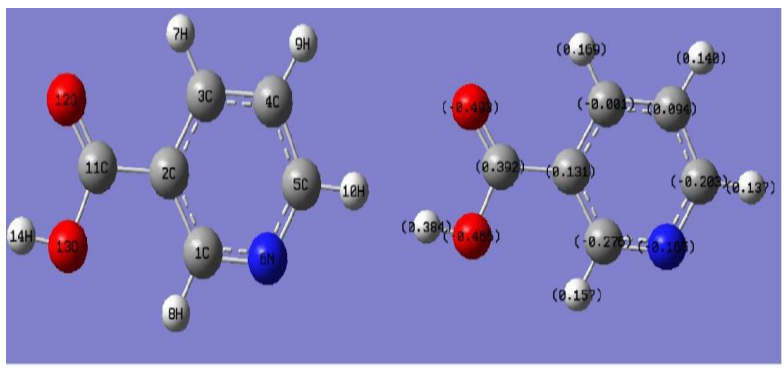

Figure 13: Optimized molecular structure (left) and mulliken charge distribution (right) of nicotinic acid.

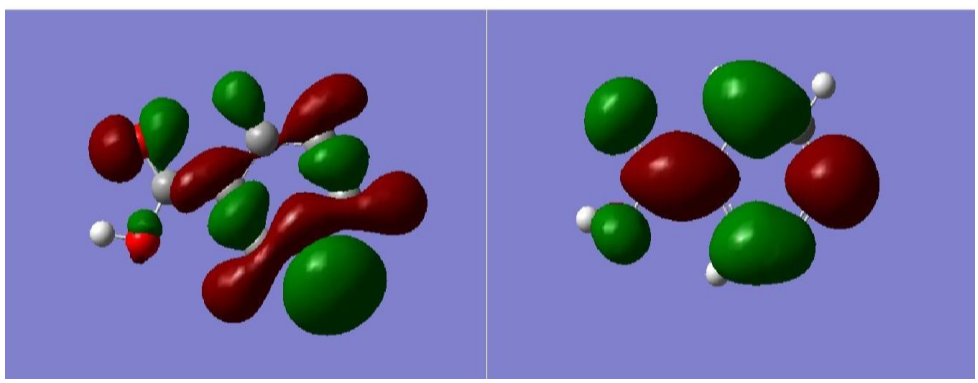

Figure 14: HOMO (left) and LUMO (right) diagrams of nicotinic acid using B3LYP/6-31+G (d, p).

Table 1: Electrochemical parameters and inhibition efficiency of NAC for copper in 3.5 wt % NaCl solution.

Concentration (mM)	E_{corr} (V/ECS)	j_{corr} ($\mu A.cm^{-2}$)	b_a (mV/dec)	b_c (mV/dec)	CR (mm/year)	R_p ($\Omega.cm^2$)	η (%)
0	-224	46.5	48	94	0.544	336.60	-
1	-259	14.6	68	208	0.170	1767.12	68.60
5	-252	14.1	68	213	0.165	1800.80	69.67
10	-300	5.6	69	138	0.065	4046.44	87.97
50	-320	9.5	79	119	0.111	2170.16	79.56

Table 2: Impedance parameters for copper in 3.5 wt % NaCl solution in the absence and presence of various concentrations of NAC at 298 K.

Concentration (mM)	R_S ($\Omega.cm^2$)	R_f ($\Omega.cm^2$)	CPE_f ($\Omega.S^n cm^{-2}$)10^{-6}	n_1	R_{ct} ($\Omega.cm^2$)	C_{dl} ($_{\mu F}.cm^2$)	n_2	η (%)
Blank	4.20	53.50	214.2	0.80	603	33.82	0.53	-
1	3.90	266.58	256.0	0.79	1621	10.75	0.61	65.2
5	4.10	411.60	107.0	0.91	1737	5.80	0.58	69.4
10	3.80	178.10	300.0	0.77	2510	3.13	0.58	75.6
50	3.86	346.10	540.0	0.70	1991	5.00	0.59	71.9

Table 3: The adsorption parameters of NAC on copper in 3.5 wt % NaCl.

$K_{ads}(10^4 M^{-1})$	$\Delta G^0_{ads}(kJ.mol^{-1})$	R^2	n
1.6	-34.09	0.9991	1.2459

Table 4: Electrochemical parameters of the corrosion of copper in NaCl 3.5 wt % solution without and with 10 mM of nicotinic acid at different temperatures.

Solution	Temperatures (K)	E_{corr}(V/SCE)	j_{corr}($\mu A/cm^2$)	η (%)
Blank	293	-225	46.8	-
	303	-260	92.2	-
	313	-271	122.0	-
	323	-269	498.0	-
10 mM NAC	293	-294	5.3	88.67
	303	-290	12.6	86.33
	313	-310	23.0	81.60
	323	-257	100.0	79.91

Table 5: Copper dissolution activation parameters in 3.5 wt % NaCl without and with 10 mM of nicotinic acid.

Solution	E_a(kJ.mol^{-1})	ΔH_a(kJ.mol^{-1})	ΔS_a(J.mol^{-1}.K^{-1})
Blank	61.27	58.60	-129.21
10 mM NAC	78.07	75.40	-90.06

Tableau 6: Quantum chemical descriptors for nicotinic acid.

Parameters	E_{HOMO}(eV)	E_{LUMO}(eV)	ΔE(eV)	μ(D)	I(eV)	A(ev)	χ(ev)	η(eV)	ΔN
Values	-7.5264	-2.1228	5.4037	0.7117	7.5264	2.1228	4.8246	2.7018	-0.0630

DISCUSSION

From the open circuit, small potential fluctuations observed during the immersion in the blank solution can be attributed to the evolution of the nature and/or surface coverage of the corrosion product film on the copper surface. In the inhibited solution, the open circuit potential evolves towards more positive values. This evolution is associated with the formation and thickening of the film at the copper surface, indicating the improvement of the corrosion resistance. On the other hand, the displacement of the corrosion potential towards negative values is considered as an indicator of surface activation (Jiménez et al., 2009). In chloride-containing media such as seawater, the decrease in the value of the open circuit potential is associated with the dissolution of the oxide native layer formed upon air exposure and the formation of CuCl complexes on the surface which does not adequately protect it (Curkovic et al., 2010). Generally, the cathodic reaction on copper in the aerated NaCl solution is a reduction reaction of dioxygen according to the following equations (Otmačić and Stupnišek-Lisac, 2003):

$$O_2 + 2H_2O + 4e^- \rightarrow 4OH^- \quad (18)$$

The process of anodic dissolution of copper in NaCl medium can be described by the following steps (Zhang et al., 2004):

$$Cu + Cl^- \rightarrow CuCl + e^- \quad (19)$$

$$CuCl + Cl^- \rightarrow CuCl_2^- \quad (20)$$

$$CuCl_2^- \rightarrow Cu^{2+} + 2Cl^- + e^- \quad (21)$$

Followed by the oxide formation

$$2CuCl_2^- + 2OH^- \rightarrow Cu_2O + H_2O + 4Cl^- \quad (22)$$

The inhibitor addition leads to the evolution of the open circuit potential towards more positive values at the end of the measurement, which suggest that the NAC protects the metal against corrosion by adsorption and the formation of a protective layer on its surface.

The polarization resistance and the inhibitory efficiency of NAC increase with the concentration of inhibitor and reach maximum values of 4046 Ω and 88% respectively for an inhibitor concentration of 10 mM and decrease thereafter. A similar behavior have been reported on copper corrosion inhibition in the cooling liquids of industrial systems in the presence of CetyltrimethylAmmonium Bromide (CTAB) (Elhousni et al., 2017). These authors have justified the decrease of the efficiency in the case of high inhibitor concentrations by the formation of an oxide and / or hydroxide layer on the surface of the material.

Others authors (Azaroual et al., 2016) attribute this behavior to an adsorbed layer saturation and to the formation of free micelles which should decrease the number of transported inhibitory molecules on the metal surface, thus causing a decrease in the inhibition efficiency.

The cathodic Tafel slope (bc) drastically changes with inhibitor addition while the anodic Tafel slope (ba) variation is very small, thus indicating that the NAC changes the dioxygen reduction mechanisms but has no significant effect on copper dissolution. The corrosion potential shifts towards more cathodic potentials with addition of different concentration of NAC. These electrochemical features suggest a cathodic character of this inhibitor (Larabi et al., 2006).

It is widely believed that a compound can be recognized as an anodic or cathodic inhibitor if the corrosion potential variation is greater than 85 mV (Scendo et al., 2012). In our study, the greatest difference between the corrosion potential in the blank solution and that with inhibitor observed is about 96 mV. This confirms that NAC acts as a cathodic inhibitor for copper in the 3.5 wt % NaCl solution.

During long term immersion test, we note that in the blank solution, the open circuit potential increases slightly up to a maximum at around 35 h of immersion and then slightly decreases. When the tests are conducted in the presence of NAC, an important shift of the potential in the first hours of immersion is observed. This shift is in good agreement with the potentiodynamic experiments and is directly linked to the action mechanism of the

inhibitor. After few hours of immersion, the open circuit potential gradually increases. This ennoblement is directly linked to the formation of a stable corrosion product film on the surface of the copper electrode (Felhősi et al., 2002).The polarization resistance during the extended immersion test increases up to 25 h in the blank solution. This increase is in good correlation with the ennoblement of the open circuit potential. The important decrease of the Rp observed After 25 h of immersion maybe associated with a change in the nature of the corrosion product film during the immersion. In the solution with inhibitor, a continuous increase of polarization resistance is observed during the immersion time. This effect can be due to the adsorption layers of NAC which have greatly reduced the rate of the copper dissolution process.

The diameter of the capacitive loops increases with the concentration of NAC indicating that the inhibition efficiency is a function of the inhibitor concentration (Elhousni et al., 2017). and a larger |Z| represents a better protection performance. The increase in the charge transfer resistance (Rct) and the efficiency (EI) of the NAC results from an increase in the surface coverage of the metal by the inhibitor. The decrease of C_{dl} is due to the adsorption of the inhibitory molecule with replacement of the water at the metal / solution interface which will cause a decrease in the local dielectric constant and / or an increase in the thickness of the double layer electric (Behpour et al., 2009). Beyond 10 mM of nicotinic acid, the charge transfer resistance decreases while the double layer capacitance increases. This means that the material becomes less protected when the amount of NAC in the solution becomes too large. The results of the effect of the concentration obtained from the polarization technique are in good agreement with those of the EIS with a small variation.

Optic microscopy images show that the grinded scratches are visible surface of the sample after in solution with NAC as freshly polished sample. The surface of sample in the blank solution is completely covered by corrosion products (Cu_2O) so that we don't see the grinded scratches. By analyzing all these images, we can note that NAC reduce effectively copper corrosion rate in 3.5 wt % NaCl solution.

Conclusion

The results obtained experimentally and theoretically lead to the following conclusions:

-Nicotinic acid (NAC) acts as a good inhibitor of copper corrosion in 3.5 wt % NaCl.

-Potentiodynamic polarization curves have indicated that this molecule acts as a purely cathodic inhibitor.

-The inhibition efficiency calculated from the electrochemical impedance spectroscopy and potentiodynamic polarization studies shows the same trend.

-The inhibition efficiency increases with increasing the concentration of NAC to reach a maximum value of 88% at a concentration of 10 mM but decreases as the temperature increases.

-The adsorption of the NAC on the surface of the copper is carried out by physical adsorption mechanism and according to the Langmuir adsorption isotherm model.

-The linear polarization gave us to note that the polarization resistance R_P increases with the immersion time indicating the stability of the protective layer formed on the surface of the metal during the 72 hours of immersion.

- Raman spectroscopy also indicates that the addition of NAC to the study solution delays the dissolution process of copper.

-There is a fairly good agreement between the calculated electronic and global reactivity parameters of nicotinic acid and the experimental results.

COMPETING INTERESTS

The authors declare that they have no competing interests.

AUTHORS' CONTRIBUTIONS

NHC and YSB conducted surveys and wrote the first draft of the article; GDD and JC are the one who validated the proposal and questionnaire; AT supervised the surveys.

ACKNOWLEDGEMENTS

The authors express great thanks to professor Juan Creus for allowing the achievement of this research in his laboratory.

REFERENCES

Aksüt A. 1997. The effect of some organic compounds on the corrosion of pure Fe, pure Cr and Fe-Cr alloys in acidic solutions. *Corrosion Science*, **39**(4): 761-774. https://doi.org/10.1016/S0010-938X(97)89340-7

Azaroual M, El Harrak E, Touir R, Rochdi A, Touhami ME. 2016. Synergistic corrosion protection for galvanized steel in 3.0% NaCl solution by sodium gluconate and cationic surfactant. *Journal of Molecular Liquids*, **220**: 549-557. https://doi.org/10.1016/j.molliq.2016.04.117

Behpour M, Ghoreishi S, Gandomi-Niasar A, Soltani N, Salavati-Niasari M. 2009. The inhibition of mild steel corrosion in hydrochloric acid media by two Schiff base compounds. *Journal of Materials Science*, **44**(10): 2444-2453. https://doi.org/10.1007/s10853-009-3309-y

Benali O, Larabi L, Tabti B, Harek Y. 2005. Influence of 1-methyl 2-mercapto imidazole on corrosion inhibition of carbon steel in 0.5 M H_2SO_4. *Anti-corrosion Methods and Materials*, **52**(5): 280-285. https://doi.org/10.1108/00035590510615776

Chidiebere MA, Oguzie EE, Liu L, Li Y, Wang F. 2015. Adsorption and corrosion inhibiting effect of riboflavin on Q235 mild steel corrosion in acidic environments. *Materials Chemistry and Physics*, **156**: 95-104. https://doi.org/10.1016/j.matchemphys.2015.02.031

Cordoba-Torres P, Mesquita T, Devos O, Tribollet B, Roche V, Nogueira RP. 2012. On the intrinsic coupling between constant-phase element parameters α and Q in electrochemical impedance spectroscopy. *Electrochimica Acta*, **72**: 172-178. https://doi.org/10.1016/j.electacta.2012.04.020

Curkovic HO, Stupnisek-Lisac E, Takenouti H. 2010. The influence of pH value on the efficiency of imidazole based corrosion inhibitors of copper. *Corrosion Science*, **52**(2): 398-405. https://doi.org/10.1016/j.corsci.2009.09.026

El Ibrahimi B, Soumoue A, Jmiai A, Bourzi H, Oukhrib R, El Mouaden K. 2016. Computational study of some triazole derivatives (un-and protonated forms) and their copper complexes in corrosion inhibition process. *Journal of Molecular Structure*, **1125** : 93-102. https://doi.org/10.1016/j.molstruc.2016.06.057

El Ouafi A, Hammouti B, Oudda H, Kertit S, Touzani R, Ramdani A. 2002. New bipyrazole derivatives as effective inhibitors for the corrosion of mild steel in 1M HCI medium. *Anti-corrosion Methods and Materials*, **49**(3): 199-204. https://doi.org/10.1108/00035590210426463

Elhousni L, Galai M, Elkamraoui FZ, Dkhireche N, Touir R, Ebn Touhami M. 2017. Corrosion and scale studies of copper used in Moroccan industrial cooling water systems. *Euro-Mediterranean Journal for Environmental Integration*, **2**(1): 12. https://doi.org/10.1007/s41207-017-0024-y

Felhősi I, Telegdi J, Pálinkás G, Kálmán E. 2002. Kinetics of self-assembled layer formation on iron. *Electrochimica Acta*, **47**(13): 2335-2340. https://doi.org/10.1016/S0013-4686(02)00084-1

Frisch MJ, Trucks GW, Schlegel HB, Scuseria GE, Robb MA, Cheeseman JR, Montgomery JA, Vreven JrT, Kudin KN, Burant JC, ….. 2003. Gaussian 03, revision A. 1. Gaussian Inc.: Pittsburgh, PA.

Gerengi H, Ugras HI, . Solomon M M, Umoren SA, Kurtay M, Atar N. 2016. Synergistic corrosion inhibition effect of 1-ethyl-1-methylpyrrolidinium tetrafluoroborate and iodide ions for low carbon steel in HCl solution. *Journal of Adhesion Science and Technology*,

30(21): 2383-2403. https://doi.org/10.1080/01694243.2016.1183407

Gomma GK, Wahdan MH. 1995. Inhibition action of n-decylamine on the dissolution of low carbon steel in sulphuric acid. *IJCT*., **2**(2) 107-110.

Jiménez YS, Gil MT, Guerra MT, Baltes L, Rosca JM. 2009. Interpretation of open circuit potential of two titanium alloys for a long time immersion in physiological fluid. *Bulletin of the Transilvania University of Braşov,* 2: 51.

Ju H, Li Y. 2007. Nicotinic acid as a nontoxic corrosion inhibitor for hot dipped Zn and Zn–Al alloy coatings on steels in diluted hydrochloric acid. *Corrosion Science*, **49**(11): 4185-4201. https://doi.org/10.1016/j.corsci.2007.05.015

Kanojia R, Singh G. 2005. An interesting and efficient organic corrosion inhibitor for mild steel in acidic medium. *Surface Engineering*, **21**(3): 180-186. https://doi.org/10.1179/174329405X49985

Khaled K, Babić-Samardžija K, Hackerman N. 2005. Theoretical study of the structural effects of polymethylene amines on corrosion inhibition of iron in acid solutions. *Electrochimica Acta*, **50**(12): 2515-2520. https://doi.org/10.1016/j.electacta.2004.10.079

Larabi L, Benali O, Harek Y. 2006. Corrosion inhibition of copper in 1 M HNO_3 solution by N-phenyl Oxalic Dihydrazide and Oxalic N-phenylhydrazide N-phenylthiosemi-carbazide. *Portugaliae Electrochimica Acta*, **24**(3): 337-346.

Li X, Deng S, Fu H. 2011. Benzyltrimethylammonium iodide as a corrosion inhibitor for steel in phosphoric acid produced by dihydrate wet method process. *Corrosion Science*, **53**(2): 664-670. https://doi.org/10.1016/j.corsci.2010.10.013

Mansouri K. 2015. Inhibition de la Corrosion de l'Acier au Carbone X-52. *Journal of Advanced Research in Science and Technology*, **2**(1): 130-138.

Martinez S, Štagljar I. 2003. Correlation between the molecular structure and the corrosion inhibition efficiency of chestnut tannin in acidic solutions. *Journal of Molecular Structure* : *THEOCHEM*, **640**(1): 167-174. https://doi.org/10.1016/j.theochem.2003.08.126

Niamien PM. 2016. Thiamine Hydrochloride as Copper Corrosion Inhibitor in 1M HNO_3. *Journal of Progressive Research in Chemistry*, **4**(1): 166-178.

Obot I, Obi-Egbedi N. 2011. Anti-corrosive properties of xanthone on mild steel corrosion in sulphuric acid: Experimental and theoretical investigations. *Current Applied Physics*, **11**(3) : 382-392. https://doi.org/10.1016/j.cap.2010.08.007

Ostovari A, Hoseinieh S, Peikari M, Shadizadeh S, Hashemi S. 2009. Corrosion inhibition of mild steel in 1M HCl solution by henna extract: A comparative study of the inhibition by henna and its constituents (Lawsone, Gallic acid, α-d-Glucose and Tannic acid). *Corrosion Science*, **51**(9): 1935-1949.https://doi.org/10.1016/j.corsci.2009.05.024

Otmačić H, Stupnišek-Lisac E. 2003. Copper corrosion inhibitors in near neutral media. *Electrochimica Acta*, **48**(8) : 985-991. https://doi.org/10.1016/S0013-4686(02)00811-3

Petrović Mihajlović MB, Radovanović M.B, Tasić ŽZ, Antonijević MM. 2017. Imidazole based compounds as copper corrosion inhibitors in seawater. *Journal of Molecular Liquids*, **225**(**C**): 127-136. https://doi.org/10.1016/j.molliq.2016.11.038

Popova A, Christov M, Deligeorgiev T. 2003. Influence of the molecular structure on the inhibitor properties of benzimidazole derivatives on mild steel corrosion in 1 M hydrochloric acid. *Corrosion*, **59**(9): 756-764. https://doi.org/10.5006/1.3277604

Scendo M, Trela J, Radek N. 2012. Purine as an effective corrosion inhibitor for

stainless steel in chloride acid solutions. *Corrosion Reviews*, **30**(1-2): 33-45. https://doi.org/10.1515/corrrev-2011-0039

Stoyanova A, Sokolova E, Raicheva S. 1997. The inhibition of mild steel corrosion in 1 M HCl in the presence of linear and cyclic thiocarbamides—Effect of concentration and temperature of the corrosion medium on their protective action. *Corrosion Science*, **39**(9): 1595-1604. https://doi.org/10.1016/S0010-938X(97)00063-2

Szauer T, Brandt A. 1981. Adsorption of oleates of various amines on iron in acidic solution. *Electrochimica Acta*, **26**(9): 1253-1256. https://doi.org/10.1016/0013-4686(81)85107-9

Tourabi M, Nohair K, Nyassi A, Hammouti B, Jama C, Bentiss F. 2014. Thermodynamic characterization of metal dissolution and inhibitor adsorption processes in mild steel/3, 5-bis (3, 4-dimethoxyphenyl)-4-amino-1, 2, 4-triazole/hydrochloric acid system. *J. Mater. Environ. Sci.*, **5**(4): 1133-1143.

Vashi R, Champaneri V. 1997. Toluidines as corrosion inhibitors for zinc in sulphamic acid. *IJCT* **4**(4) 180-184. http://hdl.handle.net/123456789/30919

Villamil RF, Corio P, Agostinho SM, Rubim JC. 1999. Effect of sodium dodecylsulfate on copper corrosion in sulfuric acid media in the absence and presence of benzotriazole. *Journal of Electroanalytical Chemistry*, **472**(2) : 112-119. https://doi.org/10.1016/S0022-0728(99)00267-3

Yingchu T, Quanzhong Z, Wenli J, Sinong C. 1996. Study on the corrosion inhibitor and fog suppressor for chemical pickling of iron and steel. *Wuhan University Journal of Natural Sciences*, **1**(2): 244-250. https://doi.org/10.1007/BF02901237

Zhang D, Gao L, Zhou G. 2004. Inhibition of copper corrosion by bis-(1-benzotriazolymethylene)-(2, 5-thiadiazoly)-disulfide in chloride media. *Applied Surface Science*, **225**(1): 287-293. https://doi.org/10.1016/j.apsusc.2003.10.016.